OPEN ACCESS Freely available online

PLOS ONE

Stretching Morphogenesis of the Roof Plate and Formation of the Central Canal

Igor Kondrychyn[1], Cathleen Teh[1], Melvin Sin[1], Vladimir Korzh[1,2]*

1 Institute of Molecular and Cell Biology, A-STAR, Singapore, Singapore, **2** Department of Biological Sciences, National University of Singapore, Singapore, Singapore

Abstract

Background: Neurulation is driven by apical constriction of actomyosin cytoskeleton resulting in conversion of the primitive lumen into the central canal in a mechanism driven by F-actin constriction, cell overcrowding and buildup of axonal tracts. The roof plate of the neural tube acts as the dorsal morphogenetic center and boundary preventing midline crossing by neural cells and axons.

Methodology/Principal Findings: The roof plate zebrafish transgenics expressing cytosolic GFP were used to study and describe development of this structure *in vivo* for a first time ever. The conversion of the primitive lumen into the central canal causes significant morphogenetic changes of neuroepithelial cells in the dorsal neural tube. We demonstrated that the roof plate cells stretch along the D–V axis in parallel with conversion of the primitive lumen into central canal and its ventral displacement. Importantly, the stretching of the roof plate is well-coordinated along the whole spinal cord and the roof plate cells extend 3× in length to cover 2/3 of the neural tube diameter. This process involves the visco-elastic extension of the roof place cytoskeleton and depends on activity of Zic6 and the Rho-associated kinase (Rock). In contrast, stretching of the floor plate is much less extensive.

Conclusions/Significance: The extension of the roof plate requires its attachment to the apical complex of proteins at the surface of the central canal, which depends on activity of Zic6 and Rock. The D–V extension of the roof plate may change a range and distribution of morphogens it produces. The resistance of the roof plate cytoskeleton attenuates ventral displacement of the central canal in illustration of the novel mechanical role of the roof plate during development of the body axis.

Citation: Kondrychyn I, Teh C, Sin M, Korzh V (2013) Stretching Morphogenesis of the Roof Plate and Formation of the Central Canal. PLoS ONE 8(2): e56219. doi:10.1371/journal.pone.0056219

Editor: Moises Mallo, Instituto Gulbenkian de Ciência, Portugal

Received September 20, 2012; **Accepted** January 7, 2013; **Published** February 7, 2013

Funding: This work was supported by the grant of the Agency for Science, Technology and Research (A-STAR) of Singapore. The funders had no role in study design, data collection and analysis, decision to publish, or preparation of the manuscript.

Competing Interests: The authors have declared that no competing interests exist.

* E-mail: vlad@imcb.a-star.edu.sg

Introduction

It is thought that neurulation ends after the neural tube is formed [1,2]. Once formed the neural tube could be divided from dorsal to ventral into the roof plate (RP), alar plate, basal plate and floor plate. The RP is an embryonic organizing center that occupies the dorsal midline of the vertebrate neural tube along the entire anterior-posterior (A–P) axis, where it produces morphogens responsible for dorsal cell fates, including BMP and Wnt [3–7]. In addition, RP also acts as a barrier preventing axons and cells migrating across the dorsal midline [8,9].

RP cells share origin with the neural crest (NC) cells, dorsal interneurons, choroid plexus and meninges [3,10–12]. While it was shown that the RP elongates during conversion of the primitive lumen into the central canal [9,13], there are no detailed studies describing this complex process *in vivo*. Historically, a relationship between the stretching of the RP and conversion of the primitive lumen into the central canal was a matter of some controversy. For example, Böhme [14] concluded that during cat development the formation of the central canal does not result directly in the formation of the dorsal glial septum (a.k.a. RP). In contrast, Sevc et al. [13] recognized interdependence of RP elongation and conversion of the primitive lumen into the central canal in rat, but suggested that the rearrangement and migration of radial glial cells is behind the transformation of the primitive lumen into the central canal. These authors along with others also recognized a role of two other factors behind conversion of the primitive lumen into central canal: cell proliferation in the neural tube and build-up of axonal pathways. Importantly, the cells lining the ventricular surface display unique organization of actin microfilaments, which disturbance results in abnormal neurulation [1,15–18]. Hence an idea of apical constriction of neuroepithelial cells of the neural plate driven by contraction of an apical meshwork of filamentous actin (F-actin) involving the vimentin-positive intermediate filaments-based cytoskeleton [19] as a main driving force of neurulation is well developed and validated experimentally [20–22]. Further to that a number of mutations affecting genes regulating organization of actin cytoskeleton cause neural tube defects and some of these mutants are characterized by the abnormal body axis. Therefore, the genes affecting actin function are under study as candidates for anencephaly-risk genes in humans [23–28]. The lack of obvious *spina bifida* phenotype in mouse mutants affecting neurulation anteriorly led to suggest that

normal actin function is critical for cranial rather than caudal neural tube closure in mice [29].

The Zic family of zinc-finger proteins is known for its crucial role in neural development and disease and, in particular, in control of neurulation (reviewed in [30–32]). Dandy-Walker malformation caused by heterozygous loss of Zic1 and Zic4 in human is defined by deficiency of the dorsal neural tube, including hypoplasia and upward rotation of the cerebellar vermis and cystic dilation of the fourth ventricle. This condition is phenocopied by similar genetic anomaly in mice [33–35]. Since it was shown that in zebrafish Zic1 and Zic4 control expression of the roof plate determinant Lmx1b, the defects in human patients deficient in these genes could be due to abnormal development of the roof plate [36]. Importantly, two other proteins of the same family, Zic2 and Zic5 are involved in neurulation during formation of the dorso-lateral hinge points, where they are required for apical F-actin and active myosin II localization and junction integrity [37]. Being lost in terrestrial vertebrates, Zic6 is probably the most mysterious member of the Zic family [38–40].

Our analysis of roof plate morphogenesis during conversion of the primitive lumen into the central canal in developing zebrafish for a first time illustrated this process in vertebrates *in vivo*. It revealed a novel mechanical role of the roof plate cytoskeleton, which attenuates the forces driving formation of the central canal. Here Zic6 plays a role in regulation of RP cytoskeleton and, in particular, attachment of these cells to the apical complex of proteins at the surface of the central canal.

Results

SqET33 Transgenic Line Expresses GFP in RP Cells

The SqET33 transgenic line used in this study has been established during *Tol2* transposon-mediated enhancer trap screen [38]. In the 3 days-old larva GFP fluorescence is detected in the neural tube along the A–P axis (Fig. 1A) largely in the dorsal aspect of the forebrain (Fig. 1B), midbrain, hindbrain (Fig. 1C) and spinal cord (Fig. 1D). In the brain, the laterally elongating processes of GFP-positive cells spread around the neural tube forming its outer envelope, the meninx (Fig. 1C). In the spinal cord, the dorsal midline GFP-positive cells elongate along the midline in ventral direction, while maintaining a contact with the primitive lumen throughout its conversion into the central canal. During this process they develop a palisade of extensions (Fig. 1D and see below). The dorsal midline GFP-positive cells are non-neuronal, since they do not express neuronal marker HuC/HuD (Fig. 1E–J). Their phenotype is reminiscent of radial glia and they express GFAP (glial fibrillar acidic protein) (Fig. 1K–M), a known marker for RP cells and astroglia in the rodent spinal cord [9]. In the zebrafish neural tube radial glia cells are mitotically active and also express GFAP [41,42]. Based on their midline position, morphology, GFAP expression and lack of neuronal markers, we concluded that they represent the RP cells.

During development the RP undergoes major morphogenetic rearrangement. The Isl1-positive sensory Rohon-Beard (RB) cells shift dorso-medially squeezing between the RP cells (Fig. 2A–I). Somata of RP cells, which were oriented medio-laterally at 24 hpf (Fig. 2A, D and J, M), by 36 hpf re-orient along the dorso-ventral (D–V) axis (Fig. 2K, N). At around 48–51 hpf RP cells start elongating (Fig. 2L, O) and by 65–66 hpf form long ventrally directed extensions (Fig. 2P–R and Movie S1). This process could be described as the uniform stretching well-coordinated along the whole A–P axis of the spinal cord. As the stretching slows down, the early (fast) phase of extension is replaced by the slow phase correlating with increase of the neural tube diameter due to growth. The length of the RP triples from 17.6 to 51.5 μm (Fig. S1). The endfeet of the central processes now form the dorsal surface of the central canal (Fig. 2Q), which is even more obvious in the SqET33-10 transgenics [38,40] expressing GFP in both roof and floor plates (Fig. 2S). It is only upon its extension that the RP may perform it barrier function and prevent cells and axons from crossing the midline (Movie S2). Unlike the RP, the floor plate cells extend much less. The palisade formed by the RP processes was observed as late as 12 dpf (data not shown), the latest time point inspected.

The Stretching of RP Correlates with Recession of the Primitive Lumen and Formation of the Central Canal

Given a connection of the RP cells to the central canal, we asked whether the RP stretching correlates with conversion of the primitive lumen of the spinal cord into the central canal. This process also known as "obliteration" of the primitive lumen was described in cat, mouse and rat [14,43,44]. It is accompanied by formation of the dorsal glial septum represented by the RP and other cells [9,13]. In zebrafish prior to 24 hpf two continuous apical membranes form along the midline and define the inconspicuous primitive lumen or neurocoel extending along all spinal cord [45]. The apical membranes present a useful landmark to study the elongation of the RP.

We asked, what is a relationship between lumen recession and extension of the RP? As lumen receded the expression of proteins representing the apical complex at the surface of the central canal - β-catenin, ZO-1 and F-actin has changed: the long slit-like domain became small, round and shifted ventrally. The processes of RP cells attached to the lumen stretched along with its closure (Fig. 3A–L). Thus, the RP stretching morphogenesis correlates with conversion of the primitive lumen into the central canal. What are the factors behind stretching of the RP? It was suggested that obliteration of primitive lumen takes place due to an increase in a number of neural cells in the spinal cord and an expansion of territory occupied by white matter [14]. Indeed, during this period a number of cells in the spinal cord increased as manifested by an increasingly dense packing of nuclei resulting from an increase in a number of cells, and the buildup of the acellular white matter in the lateral aspect of the neural tube (Fig. 3M–T). In result, the whole cellular territory acquired the wedge shape extended along the D–V axis. Thus, F-actin constriction, cell proliferation and buildup of white matter correlate with the rearrangement of the primitive lumen into central canal and stretching of the RP cells. These could be the mechanistic factors behind late neurulation in zebrafish similar to that in mammals.

Genetic Analysis of RP Elongation

It was shown that mutations affecting components of the Nodal and Hedgehog (Hh) signaling pathways disturb formation of the neurocoel and floor plate [46–49]. We asked whether these and some other pathways contribute in RP elongation. Hence, we analyzed this process in the spinal cord of mutants affecting Hh (*smu* and *syu*), Nodal (*oep*), Notch (*mib*) and Par (*pard6γb*, see below) functions at the background of SqET33 transgenics. Mutations affecting the Hh and Nodal signaling caused deformation of the body axis in *smu*, *syu* and *oep* mutants (curved down trunk). However, the GFAP-positive radial scaffold is formed and the RP stretched, although the overall length of RP processes was shorter in comparison with controls (Fig. S1). In contrast, *mib* mutant showed the curved up body axis (Fig. 4A), loss of anterior RP cells (Fig. 4A′) as well as an absence of RP stretching (Fig. 4B, C) and GFAP-positive radial scaffold (Fig. 4D–I). Thus, the reduction of the primitive lumen and extension of the RP in zebrafish correlates

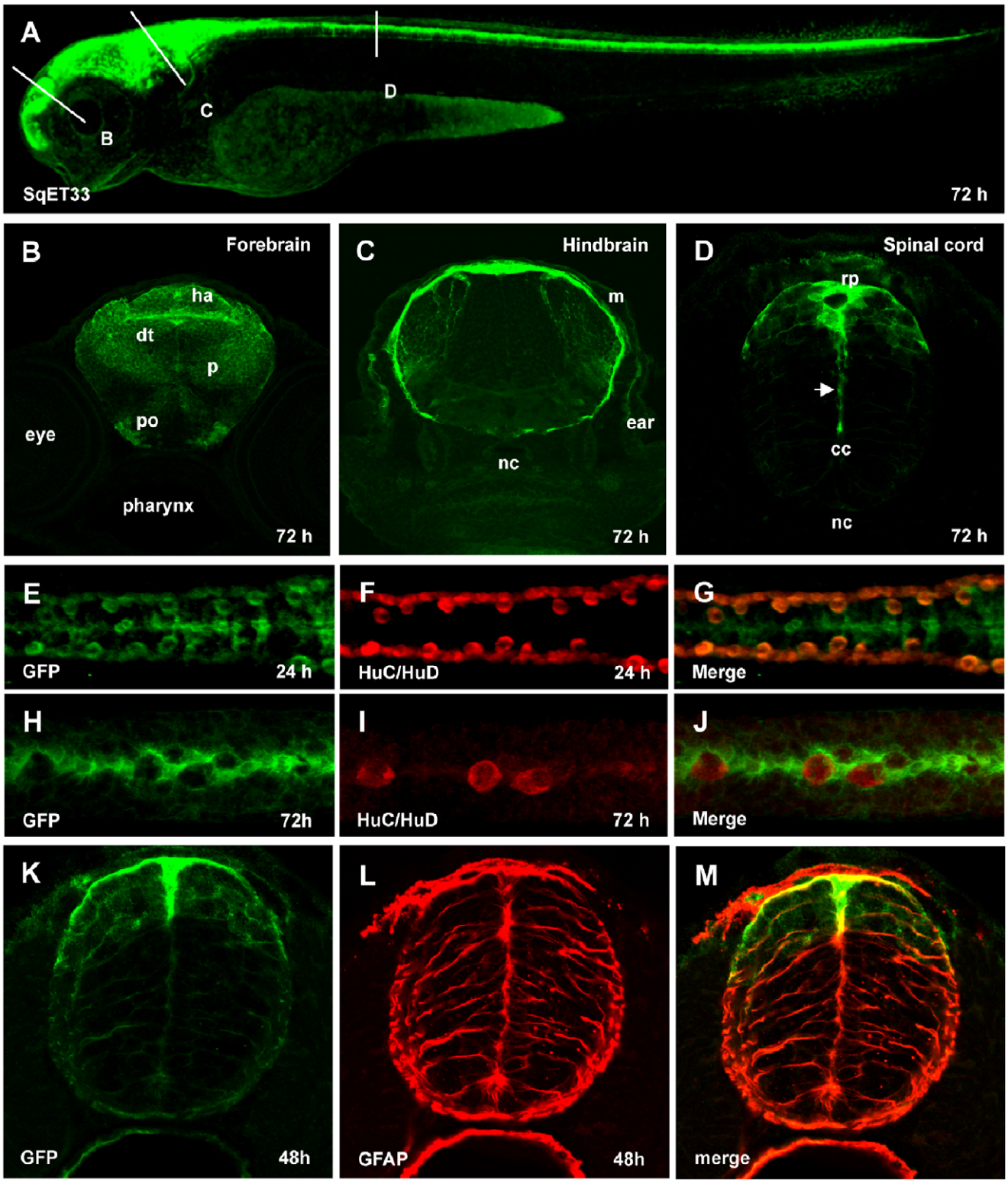

Figure 1. Characterization of SqET33 transgenic line. (A), Confocal image of 3 dpf larva of SqET33 line, lateral view. Dashed lines depict the position of transverse sections shown in B–D. (B–D), transverse sections, immunofluorescent staining with anti-GFP antibodies. Arrow indicates the elongated central process of the roof plate cell. (E–J), whole-mount immunofluorescent staining with anti-GFP (midline RP cells and lateral dorsal interneurons) and anti-HuC/HuD (lateral dorsal neurons) antibodies, dorsal view of spinal cord. (K–M), immunofluorescent staining with anti-GFP (green) and anti-GFAP (red) antibodies, transverse section of the spinal cord. Abbreviations: cc, central canal; dt, dorsal thalamus; ha, habenula; m, meninx; nc, notochord; p, pallium; po, preoptic area; rp, roof plate.
doi:10.1371/journal.pone.0056219.g001

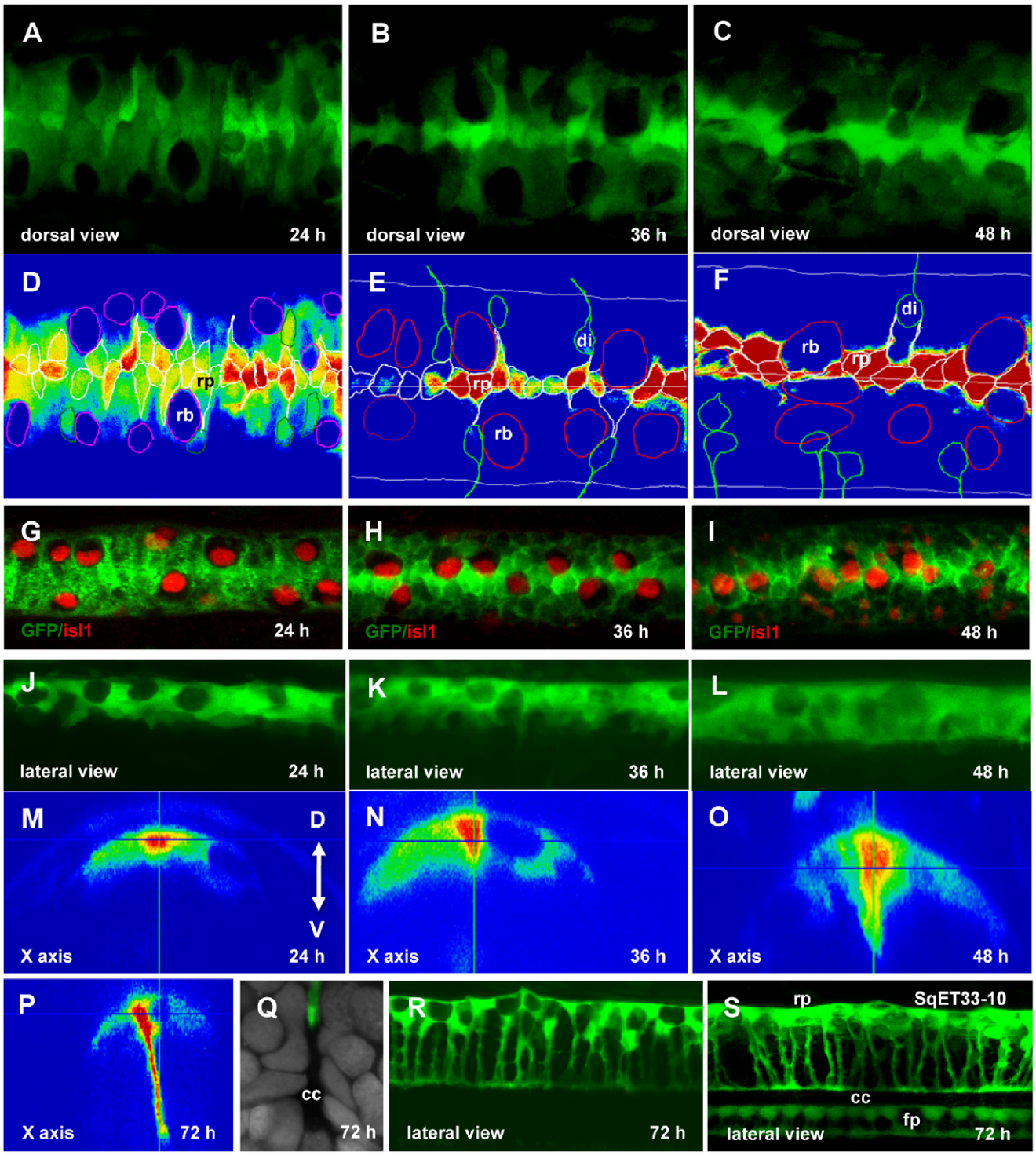

Figure 2. Re-orientation of the RP cells. Confocal images of the spinal cord of SqET33 line at different developmental stages (A–C, dorsal view, J–L, R, lateral view, M–P, orthogonal optical sections) and outline of the dorsal cells (D–F) superimposed onto the GFP intensity chart. Note that RB cells undergo the lateral-medial displacement. (G–I), Whole-mount immunohistochemistry detecting Islet1 in RB cells (red, nuclei), dorsal view of the spinal cord. (Q), Transverse section of the spinal cord at high magnification showing a fine structure of the central canal. RP process is stained with anti-GFP (green) and nuclei are counterstained with DAPI (grey). (S), Confocal image of the spinal cord of SqET33-10 line expressing GFP in the roof and floor plates, lateral view. Abbreviations: cc, central canal; di, dorsal interneurons; fp, floor plate; rb, Rohon-Beard cells; rp, roof plate cells.
doi:10.1371/journal.pone.0056219.g002

with formation of the GFAP-positive radial scaffold similar to that in mammals [13]. In contrast, the direction of the body curvature in different mutants shows no correlation with the RP extension.

Glyt1 (Slc6a9) is a glycine transporter expressed in non-neuronal cells that face the lumen of the developing spinal cord [50]. The ventricular zone contains radial glial cells that function

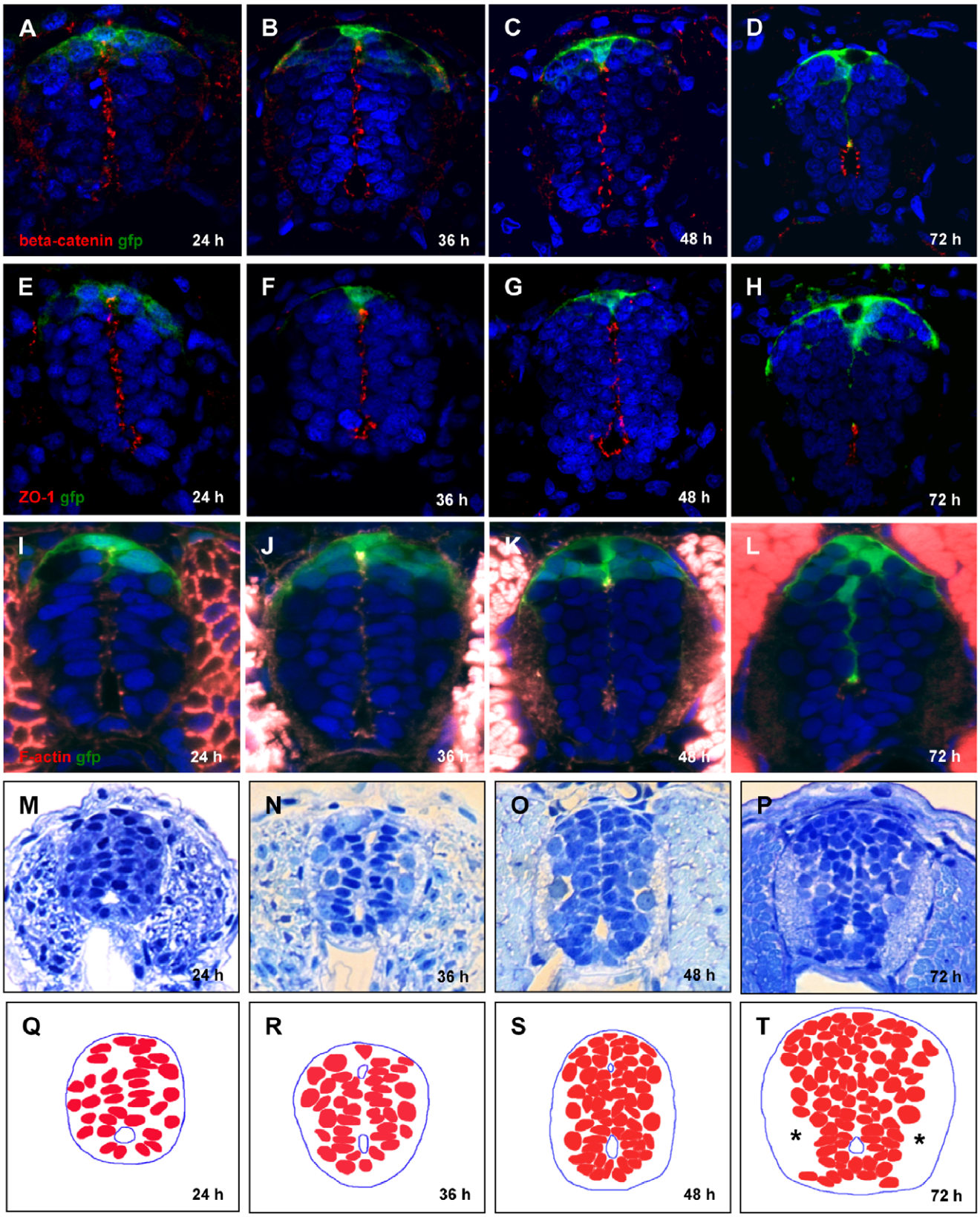

Figure 3. Conversion of primitive lumen into central canal. (A–L), Contraction of opposed apical surfaces reflects recession of the primitive lumen into a central canal between 24 and 72 hpf. Immunofluorescent staining by a combination of anti-GFP with anti-β-catenin antibody (A–D), anti-ZO-1 antibody (E–H), and phalloidin that detects F-actin (I–L). Increase in cell number and build-up of axonal tracts (*), plastic transverse sections of the spinal cord (M–P). (Q–T), Schematics corresponding to (M–P) showing cell nuclei.
doi:10.1371/journal.pone.0056219.g003

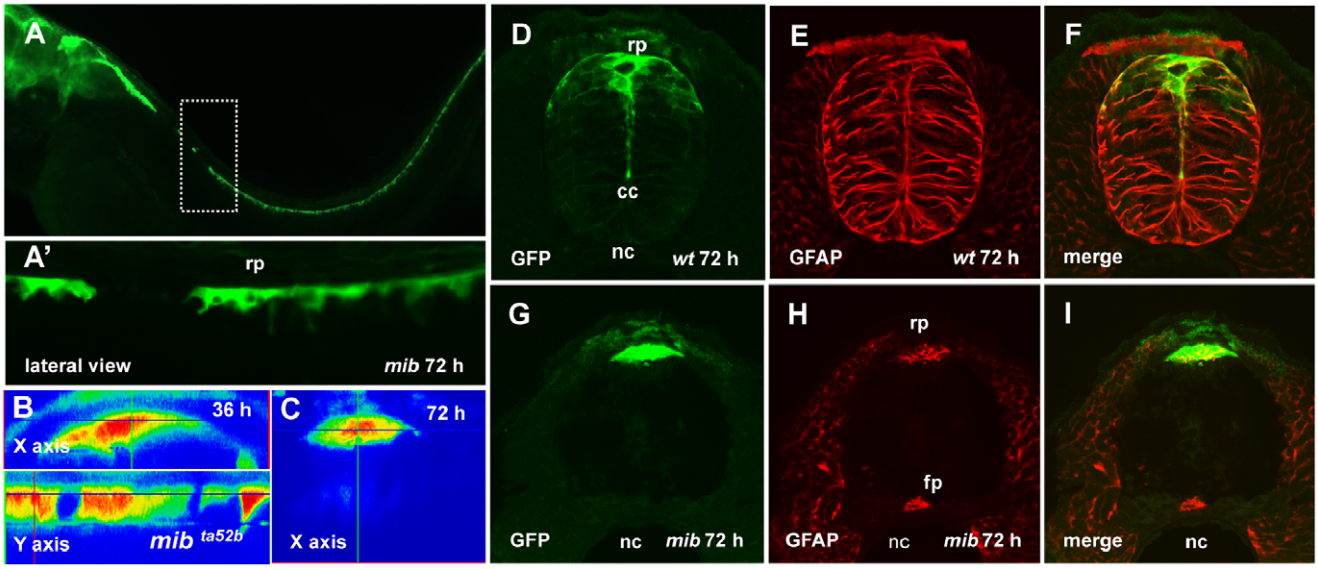

Figure 4. The roof plate formation in the *mib* mutant. (A), Confocal images, lateral view of the spinal cord of *mib* mutant, 72 hpf. Dashed rectangular shows the magnified in (A') region of the spinal cord with the absence of GFP-positive RP cells. (B, C), the orthogonal optical sections of confocal images of the spinal cord of *mib* mutant illustrate lack of the roof plate extension between 36 and 72 hpf. Immunofluorescent staining of the transverse sections of spinal cord using anti-GFP (green) and anti-GFAP (red) antibodies; wild-type embryo (D–F) and *mib* mutant (G–I).
doi:10.1371/journal.pone.0056219.g004

as neural stem cells [51–52]. Glycine is a crucial element in rapid proliferation of cancer cells [53–55]. During development the expression domain of *glyt1* shifts ventrally in parallel with conversion of the primitive lumen into the central canal as illustrated by RP extension (Fig. 5A–D) and dynamic expression of β-catenin (Fig. 5E–J). At 72 hpf *glyt1* is expressed in cells lateral to the central canal, i.e. immediately adjacent to the ventral portion of RP extensions (Fig. 5I, J).

The mutation in *pard6γb* gene disturbs formation of the central canal resulting in multiple lumens [56]. We developed recently another mutant allele of this gene - transgenics SqKR15 line that carry the *Tol2* transposon insertion in *pard6γb* gene [57]. As expected in SqKR15 homozygote embryos *glyt1* was expressed as multiple short domains in illustration of abnormal central canal presented as multiple small lumens. In parallel, the RP failed to stretch (Fig. 5K–M). This illustrated the fact that abnormal conversion of the primitive lumen into central canal affects stretching morphogenesis of the RP.

SqET33 carries a single transposon insertion in *zic6* 3′UTR. In this line GFP expression recapitulates that of *zic6* [38] expressed in the RP (Fig. S2). We asked whether this gene plays a role in RP development. In absence of the Zic6 mutant we used the morpholino (MO)-mediated loss-of-function (LOF) approach. Zic6 morphants developed the curled-down body axis (Fig. S3) and some of them consistently showed the characteristic "gaps" in the palisade of the RP extensions at the level of extended yolk, where extensions of the RP cells were short and their distribution abnormal (Fig. 6A, B). In parallel, the GFAP-positive radial processes failed to form similar to that in *mib* mutants (Fig. 6C–F).

Some understanding of the mechanism involved in formation of "gaps" in the roof plate of Zic6 morphants came in result of analysis of distribution of *glyt1* mRNA and β-catenin. Intuitively, we expected to find the expression domains of GFP and *glyt1* in close proximity to each other all along the A–P axis, including the "gaps". Contrary to these expectations at the "gap" level the two markers separated with domain of *glyt1* expression shifted ventrally and short processes of RP cells found in abnormally dorsal position (Fig. 6G–P). in parallel, GFP expression in the roof plate was no longer found to be associated with β-catenin signal with the latter being displaced ventrally (Fig. 6K, L and O, P). This phenotype is consistent with a breakdown of the attachment of RP processes to the central canal and their displacement dorsally due to contraction in parallel with displacement of the *glyt1* and β-catenin domains of expression ventrally.

Several features of the morphant phenotype - the curled body axis, failure of RP extension and GFAP expression as well as changes in *glyt1*/β-catenin expression were consistent with defects of the cytoskeleton in RP cells. Hence we performed a small-scale screen for inhibitors of various signaling pathways in attempt to mimic the effect of Zic6 LOF. The inhibitors were injected into the hindbrain ventricle at 30 hpf from where they spread throughout the whole ventricular system and central canal [58]. The defects in RP morphology were scored at 72 hpf. Only embryos injected with the inhibitor of Rho-associated protein kinases (Rock1 and Rock2) - Y27632 [59–61] showed somewhat similar phenotype (Fig. 7A, B). Similar to that in Zic6 morphants, an inhibition of Rock caused a failure of RP extension in parallel with changes in distribution of proteins of the apical protein complex (F-actin, Fig. 7 C–E) and distribution of *glyt1* expression (Fig. 7F, G). The difference was manifested by much larger gaps in the roof plate palisade or complete failure of RP extension.

Rock activation is known to result in a concerted series of events at the level of cytoskeleton that promote force generation and morphological changes in particular during neurulation [60]. An application of inhibitors blocking individual contractile proteins (F-actin, myosin-2, tubulin) that were shown earlier to affect neural tube closure [60] failed affect extension of the RP (Table S1). This could be due to insufficient penetration of these compounds into the lumen of the neural tube resulting in their suboptimal concentration or due to redundancy at the level of individual contractile proteins involved in this process.

Here we demonstrated that extension of the RP cells requires their attachment to the apical complex of proteins at the surface of the central canal and depends on activity of Zic6 and Rho-

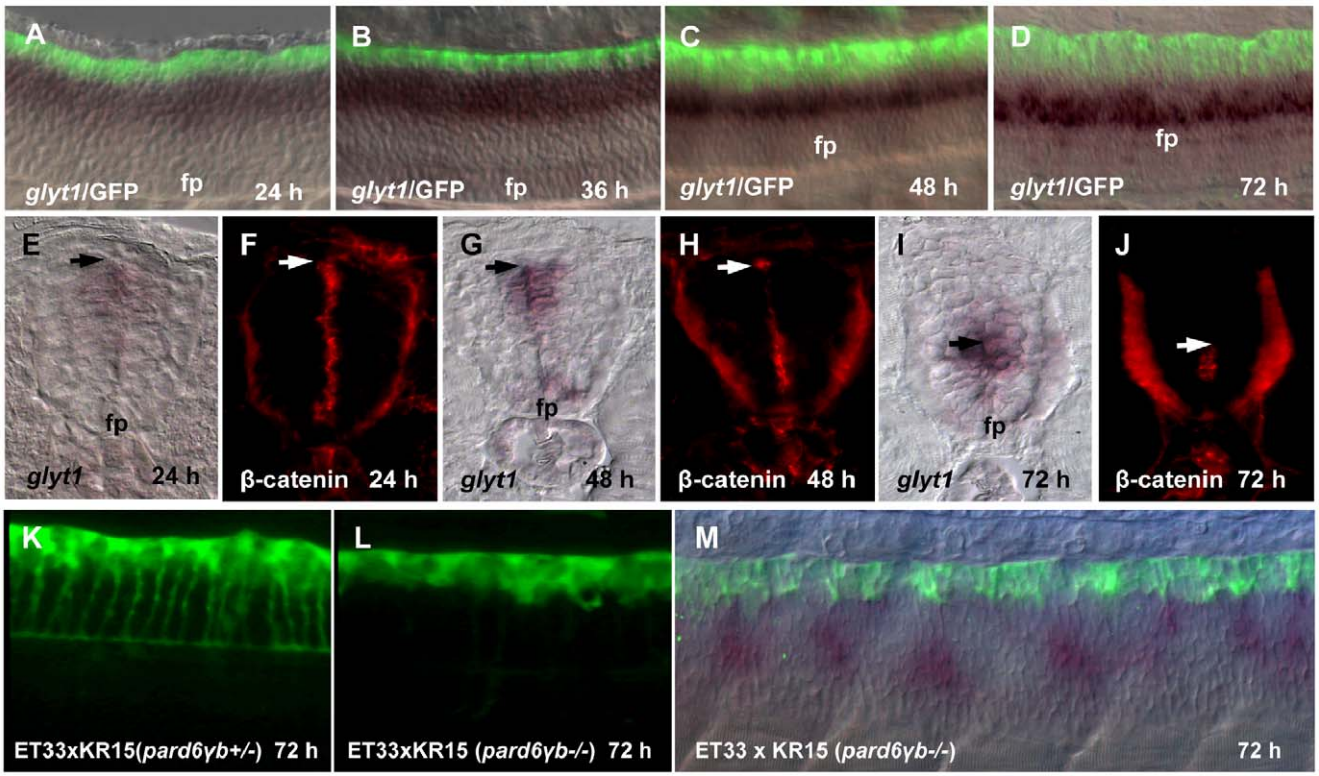

Figure 5. Growth of the RP processes correlates with a shift of *glyt1* expression along D–V axis. (A–D), Double whole mount *in situ* hybridization (*glyt1*, dark purple) and immunostaining (GFP, green). *glyt1* is expressed in the midline glial cells except RP; GFP is expressed in the RP cells. (E–J), Whole mount *in situ* hybridization (*glyt1*, dark purple) and immunostaining (β-catenin, red), the transverse sections of the spinal cord. The arrow shows an approximate position of attachment of the RP process to the apical surface of central canal. Confocal images of the spinal cord of *pard6γb* heterozygote (K) and *pard6γb* mutant (L) transgenic fish. (M), double whole mount *in situ* hybridization (*glyt1*, dark purple) and immunostaining (GFP, green) of *pard6γb* mutant. Abbreviation: fp, floor plate.
doi:10.1371/journal.pone.0056219.g005

associated protein kinase. The resistance of the RP cytoskeleton attenuates ventral displacement of the central canal during a process of reduction of the primitive lumen (Fig. 8).

Discussion

The RP is an evolutionarily conserved dorsal organizing center of the embryonic neural tube and the midline barrier [3,8–10]. The RP development was studied in birds and mammals, but details of morphogenesis of these cells are not fully understood in particular in a context of conversion of the primitive lumen into the central canal. Here we used several zebrafish transgenics with expression of cytosolic GFP in the RP to study for the first time the morphogenesis of the RP cells *in vivo* and analyze the factors involved. The deficiency of the roof plate cells adhesion results in interruption of conversion of the primitive lumen into the central canal.

The RP undergoes well-coordinated "stretching" morphogenesis along the whole extent of the spinal cord (Movie S1) in correlation with closure of the primitive lumen. This probably is the first morphogenetic event coordinated within the whole spinal cord. Noteworthy that initiation of fast RP extension correlates with hatching (48–52 hpf) [62]. Our observations were made on larvae that were dechorionated prior to imaging. Hence the reduction of the primitive lumen and stretching of the RP are independent of the hatching *per se*. These developmental events must be regulated by distinct genetic mechanisms.

The stretching morphogenesis of the RP takes place under the influence of opposing forces. Here a constriction of the apical belt of F-actin along with cell overcrowding and lateral pressure of expanding axonal pathways (i.e. pull-push force) drives an elongation of the cellular (grey) area of the neural tube along the D–V axis. This correlates with conversion of the primitive lumen into a central canal. The resistance (i.e. dragging force) of cytoskeleton of the RP and other cells of the neural tube undergoing visco-elastic stretching attenuates this process. In zebrafish this process is rather asymmetrical with much more significant elongation of the roof plate comparing to the floor plate. This is similar to that in cat, where cell proliferation along with a buildup of axonal tracts significantly contributes into dorsal closure ("obliteration") of primitive lumen with little extension of the floor plate [14]. Similar developmental scenario takes place in the spinal cord in camel [63]. This is somewhat different from that in mice and rat, where the closure of primitive lumen happens both dorsally and ventrally [13,41]. In this respect, this process in zebrafish is more reminiscent of that in the cat and camel.

Based on analysis of primitive lumen closure in mammals, Sevc et al. [13] proposed an active role of radial glia in the transformation of the primitive lumen into the central canal. The RP morphogenesis should be considered in view of interaction of two opposing forces, where the cytoskeleton in cells that elongate counteracts the pull-push forces driving conversion of the primitive lumen into the central canal. Hence mechanically a role of RP cells manifests itself through cytoskeleton resistance opposing the factors behind the push-pull force. To form an integrated layer the

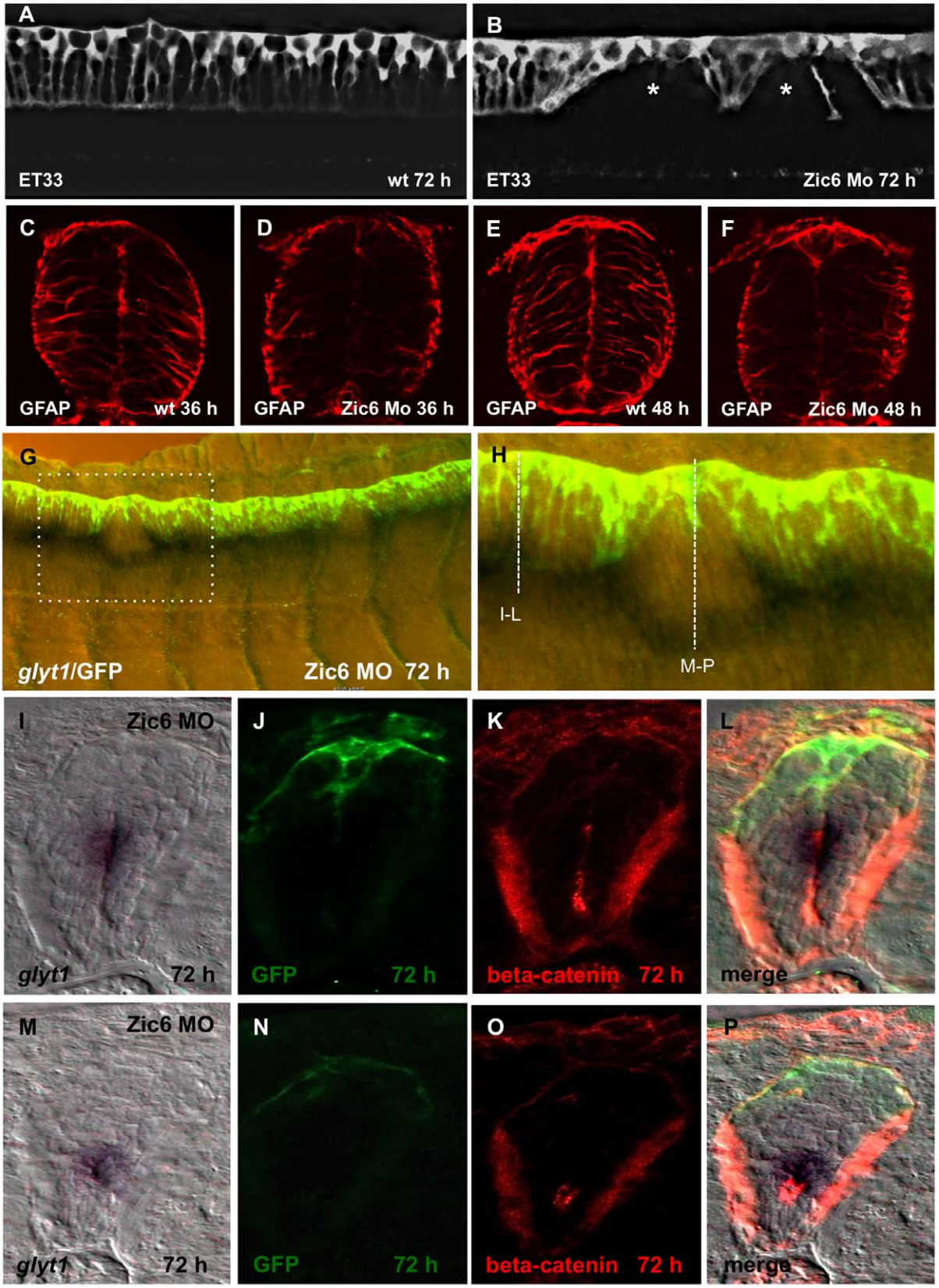

Figure 6. Zic6 is required for development of the radial glial scaffold and attachment of RP cells to the dorsal surface of central canal. Confocal images, lateral view of the spinal cord, 72 hpf. SqET33, control (A) and Zic6 morphant (B). The asterisk indicates the "gaps" in the palisade of RP cells. (C–F), Immunostaining of the transverse sections of the spinal cord with anti-GFAP antibody. (G), Double whole-mount *in situ* hybridization (*glyt1*, dark purple) and immunostaining (GFP, yellow/green) of the spinal cord Zic6 morphant. The dashed rectangular marks the

magnified region (H). The dashed lines show the approximate positions for the transverse sections shown in (I–P). (I–P), distribution of *glyt1*, β-catenin and GFP in two positions in the spinal cord of Zic6 morphants shown in H, corresponding to I–L and M–P.
doi:10.1371/journal.pone.0056219.g006

cells lining the ventricular surface rely on their cytoskeleton and the apical complex of proteins, including F-actin, ZO-1 and β-catenin [1,15–18]. Zic6 fits this model nicely. Other proteins of the Zic family either control formation of the roof plate (Zic1 and Zic4) or are involved in neurulation during formation of the dorso-lateral hinge points (Zic2a and Zic5), where they are required for junction integrity [36,37]. Perhaps, during closure of the primitive lumen and formation of the central canal Zic6 plays a role in regulating the cytoskeleton of RP. The redundancy of Zic proteins may explain why a "gap" phenotype was detected only in some embryos. This explanation is also in line with conservation of the neurulation mechanism involving closure of the primitive lumen and formation of the central canal during evolution despite disappearance of Zic6 in tetrapods [13,32,37–39,64].

Our data support a model suggesting that during conversion of the primitive lumen into central canal the resistance of RP cytoskeleton, and by extension that of other cells in the dorsal neural tube, which are connected by the apical complex of proteins at the surface of the central canal, is insufficient to resist the factors behind the pull-push force causing stretching of the RP (Fig. 8). The failure of adhesion of the RP cells to the apical complex of proteins at the surface of the central canal in Zic6 morphants causes a breakdown between cytoskeleton and apical junction resulting in displacement of the roof plate dorsally and the central canal ventrally. It also weakens the cytoskeleton of the spinal cord resulting in curling of the body axis. This elegantly illustrates a tug-of-war between different axial structures behind straightening of the body axis and demonstrates the novel mechanical function of the roof plate during formation of the body axis.

Materials and Methods

Fish were maintained, mated and raised as described [65] according to the rules of the IMCB fish facility and the Biopolis IACUC protocol #090430. Embryos were kept at 28.5°C and staged according to Kimmel et al. [62]. For anesthetizing, 0.16 mg/ml of buffered 3-aminobenzoic acid ethyl ester (Tricaine, Sigma), containing Tris buffer, pH7, was used. To inhibit pigment formation, 0.2 mM 1-phenyl-2-thiourea was added to embryo medium after 16 hours of post fertilization (hpf).

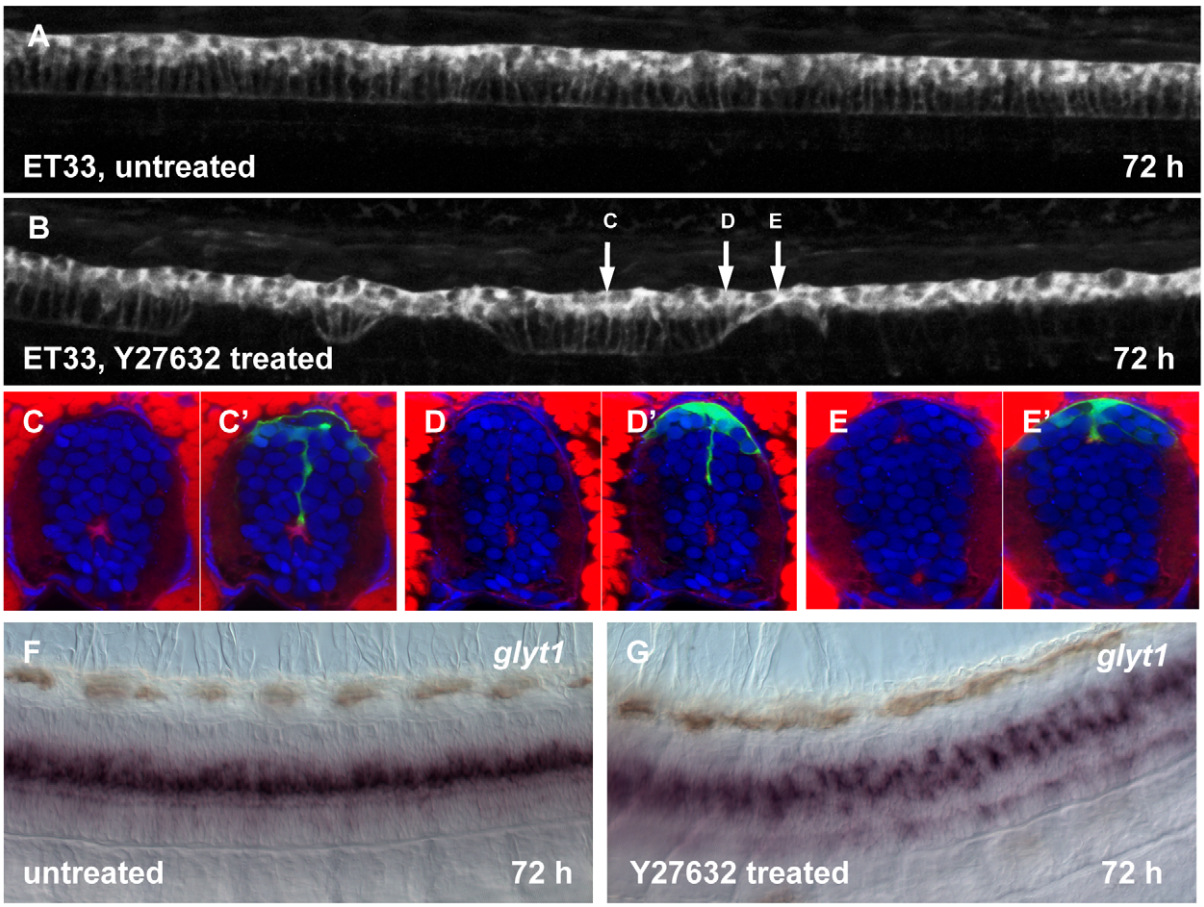

Figure 7. Effect of Rock inhibition on the RP morphogenesis. Confocal images of 72 hpf larva, untreated (A) and after Y-27632 injection into hindbrain ventricle at 30 hpf (B). The arrows show an approximate position of the transverse sections. (C–E'), transverse sections of the spinal cord of larva, treated with Y-27632. Immunofluorescent staining with anti-GFP (green) and phalloidin (red). Whole mount *in situ* hybridization with *glyt1* antisense RNA probe, control (F) and after treatment with Y-27632 (G).
doi:10.1371/journal.pone.0056219.g007

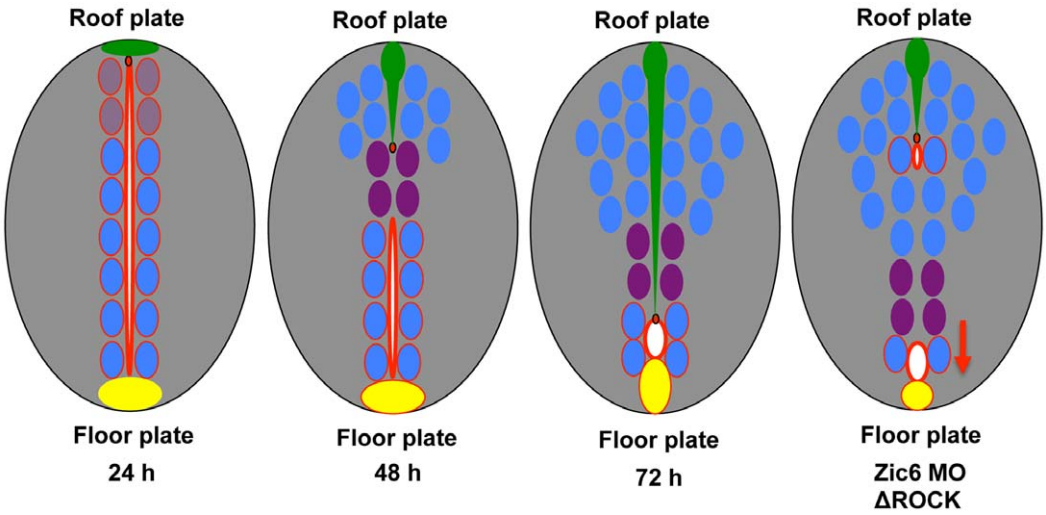

Figure 8. Critical events during stretching morphogenesis of the RP in zebrafish. The scheme illustrates the stretching morphogenesis of the RP, which takes place during late neurulation in correlation with reduction of the primitive lumen into the central canal. In zebrafish this process depends on activity of Zic6 and Rock.
doi:10.1371/journal.pone.0056219.g008

Transgenic and Mutant Fish Lines

In this study we used the following transgenic lines: SqET33, SqET33-10 and Sq33-E20, generated during enhancer trap screen [11,38,40]. Several lines with different mutant background were generated by mating the SqET33 line with heterozygous mutant partners. The offspring were raised and heterozygous transgenic lines carrying the appropriate mutated allele were identified by mating with given mutant. The following alleles of zebrafish mutants were used in this study: *mib*^{ta52b}, *oep*^{z1}, *smu*^{b641}, *syu*^{t4} and SqKR15 harboring transposon insertion in *pard6γb*, which represents an independent mutant allele affecting this gene [57,66–69].

Cloning of *glyt1* Gene

Full-length cDNA for *glyt1* gene was amplified using primers: *forward* 5′-AGA CTG ACC TGG AGA GTG TTT TGC C-3′ and *reverse* 5′-CAA TGC GCT ATA TAC ACA ATG CGT G-3′. Resulting PCR product was cloned into pGEM-TEasy vector (Promega).

Antibodies

The following primary antibodies were used: mouse monoclonal anti-GFP (clone B-2, Santa Cruz Biotechnology), anti-β-catenin (clone 15B8, Sigma), anti-GFAP (clone G-A-5, Sigma) and anti-ZO1 (gift from Dr. Drummond, Harvard University, USA); rabbit polyclonal anti-Isl-1 [70] and anti-GFP (BD Living Colors, Clontech). Secondary antibodies from Molecular Probes were used: Alexa Fluor 488-conjugated goat anti-mouse and anti-rabbit $F(ab)_2$ fragments and Alexa Fluor 543-conjugated goat anti-mouse and anti-rabbit $F(ab)_2$ fragments.

Whole-mount *in situ* Hybridization

Embryos were fixed in Histochoice Tissue Fixative MB (Amresco, USA) overnight at room temperature, washed in PBST and treated with 3% H_2O_2 for 15 min. Hybridization was carried out in hybridization solution containing 5% dextran sulphate at 65°C. After stringency wash, the digoxigenin-labelled RNA probe was detected with anti-digoxigenin antibody, conjugated with alkaline phosphatase (Roche). Staining was developed in detection buffer containing 2% polyvinyl alcohol (Sigma).

Whole-mount Immunofluorescent Histochemistry

Embryos were fixed in Histochoice Tissue Fixative MB (Amresco, USA) for 2 hours at room temperature, washed 3 times for 15 min in PBST (1 x PBS, 0.1% Tween-20) and permeabilized in 0.1% Triton X-100 in 0.1% sodium citrate for 30 min. Then embryos were incubated for 2 hours in 5% Blocking Reagent (Roche) in MAB (150 mM maleic acid, pH 7.5, 100 mM NaCl, 0.1% Tween-20). Embryos were incubated with primary antibodies (1:200) overnight at 4°C, washed 4 times for 30 min in MAB and incubated with secondary antibodies (1:500) for 6 hours at room temperature in darkness. Finally, embryos were extensively washed in PBS and kept in 50% glycerol in PBS until being monitored under fluorescent or confocal microscope.

Immunofluorescent Histochemistry

Embryos were fixed in Histochoice Tissue Fixative MB (Amresco, USA) overnight at 4°C, washed 3 times for 15 min in PBST and embedded in 2% agar (Difco, USA) in PBS. For F-actin staining, embryos were fixed with 4% paraformaldehyde in actin stabilizing buffer (50 mM PIPES, 150 mM KCl, 1 mM $CaCl_2$, 1 mM EGTA, pH 6.5) overnight at 4°C. Before cryosectioning, agar blocks were kept in 30% sucrose in PBS overnight at 4°C. Cryosections with thickness 15μm were done using Leica cryostat. Sections were washed 3 times for 5 min in PBST, permeabilized for 30 min in PBS containing 0.1% Triton X-100 and1% DMSO, blocked in blocking solution (5% BSA and 0.05% Tween-20 in PBS) for 1 hour and incubated with primary antibodies (1:200) for 1 hour in humid chamber at room temperature. Then sections were rinsed 3 times for 5 min in PBST and incubated with secondary antibodies (1:500) for 1 hour. F-actin was detected using phalloidin-Alexa Fluor 635 (Molecular Probes) according to manufacture's protocol. Finally, sections were washed 3 times for 5 min in PBST and nuclei were counterstained with DAPI for 5 min.

Plastic Sectioning

Embryos were fixed in 4% glutaraldehyde in 25 mM sodium phosphate buffer (pH 6.8) for 4 hours at room temperature, washed twice in phosphate buffer for 30 min and dehydrated through ethanol series (20%, 40%, 60%, 80% and 99%) for 30 min. Then embryos were infiltrated and embedded with Historesin (Leica) according to manufacture. Plastic sections with thickness 5 μm were done using Leica machine. Tissue sections were stained with toluidine blue for 1 min.

Confocal Microscopy

Confocal imaging of zebrafish embryos was performed using the Zeiss LSM510 confocal microscope. The time-lapse imaging was performed using the Olympus FluoView FV1000 confocal microscope equipped with temperature controlling chamber. Dechorionated embryos were mounted in 0.5% low-temperature melting agarose in an imaging chamber prepared from a modified Petri dish. The embryo medium was supplemented with Tricaine to inhibit movement of fish. Embryos held in the imaging chamber maintained heartbeat and circulation throughout the imaging period. Two-dimensional or three-dimensional reconstructions of image data were prepared using the standard LSM or Olympus software package and ImageJ (NIH, USA).

Morpholino Injection

Zic6 knockdown was performed using a translation-blocking antisense morpholino oligonucleotide (MO) purchased from Gene Tool, LLC. The MO sequence was 5′-TTG GTT GAT TTG CCA AGC CCT CAG C-3′. A mismatch antisense MO with the following sequence 5′-TTG cTT GAT gTG CCt AGC tCT gAG C-3′ was used as a control. Embryos were injected with 2.1 ng Zic6 MO or 8.5 ng Zic6 mismatch MO at the 1–2 cell stage. For the rescue experiments Zic6 MO was co-injected with 25 pg of *zic6* mRNA without morpholino binding site. Results of morpholino experiments are presented in Figure S3.

Ventricular Injections of Small Molecule Inhibitors

Injection of small molecule inhibitors in specific concentration (see Table S1) was performed at 30 hpf into the hindbrain ventricle from where it spread with the cerebrospinal fluid into the central canal [58] and their effect on the roof plate cells elongation was scored at 72 hpf under compound fluorescent microscope.

Supporting Information

Figure S1 Mutant analysis of RP formation. Immunofluorescent staining of the transverse sections of the spinal cord of *smu* (A-C) and *syu* (D-F) mutants. Confocal images of the spinal cord of *smu* (M), *syu* (N) and *oep* (O) mutants at 72 hpf. Orthogonal optical sections of the confocal images of the spinal cord of *smu* (G, J), *syu* (H, K) and *oep* (I, L) mutants at different developmental stages. (P), The length of RP process in different mutants.
(TIF)

Figure S2 Expression pattern of *zic6*. (A), RT-PCR analysis of *zic6* expression. Each even line represents negative control (minus RT). MBT, mid-blastula transition. (B–E), Whole-mount *in situ* hybridization with *zic6* RNA probe at different developmental stage. c, cerebellum; de, diencephalon; h, hindbrain; m, midbrain; mhb, midbrain-hindbrain boundary; ot, optic tectum; rp, roof plate; s1, approximate position of the 1st somite; t, thalamus; te, telencephalon.
(TIF)

Figure S3 Zic6 morpholino knock-down experiments. (A–C), The morphants developed the curled-down body axis, the abnormal hindbrain reminiscent of that in *mib* mutants, cardiac edema. (D), Zic6 morpholino knock-down experiments (Exp 1 to 3) and rescue experiment (Exp 4). The roof plate "gap" phenotype was scored at 72 hpf in separate experiments (Exp 5 to 8, the numbers of assessed embryos are shown in brackets).
(TIF)

Table S1 Effect of small molecule inhibitors on roof plate extension.
(DOC)

Movie S1 The low-resolution movie shows the spinal cord of SqET33 zebrafish (36–72 hpf) with coordinated stretching of the roof plate.
(MOV)

Movie S2 The high-resolution movie shows the spinal cord of SqET33-E20 zebrafish (47–65 hpf) with coordinated stretching of the roof plate. It illustrates the barrier function of the spinal cord as shown by failed attempts of the GFP-positive neuron to cross the midline.
(MOV)

Acknowledgments

We thank personnel of the IMCB fish facility for maintenance of fish lines, Drs. Randy Peterson, Robert Robinson and Dmitry Bulavin for inhibitors, Dr. J.-P. Thiery for constructive suggestions.

Author Contributions

Conceived and designed the experiments: IK VK. Performed the experiments: IK CT MS. Analyzed the data: IK MS VK. Contributed reagents/materials/analysis tools: CT. Wrote the paper: IK VK.

References

1. Karfunkel P (1974) The mechanisms of neural tube formation. Int Rev Cytol 38: 245–271.
2. Colas JF, Schoenwolf GC (2001) Towards a cellular and molecular understanding of neurulation. Dev Dyn 221: 117–145.
3. Lee KJ, Jessell TM (1999) The specification of dorsal cell fates in the vertebrate central nervous system. Annu Rev Neurosci 22: 261–294.
4. Liem KF Jr, Tremml G, Jessell TM (1997) A role for the roof plate and its resident TGFbeta-related proteins in neuronal patterning in the dorsal spinal cord. Cell 91: 127–138.
5. Millen KJ, Millonig JH, Hatten ME (2004) Roof plate and dorsal spinal cord dI1 interneuron development in the dreher mutant mouse. Dev Biol 270: 382–392.
6. Muroyama Y, Fujihara M, Ikeya M, Kondoh H, Takada S (2002) Wnt signaling plays an essential role in neuronal specification of the dorsal spinal cord. Genes Dev 16: 548–553.
7. Shimamura K, Hirano S, McMahon AP, Takeichi M (1994) Wnt-1-dependent regulation of local E-cadherin and alpha N-catenin expression in the embryonic mouse brain. Development 120: 2225–2234.
8. Butler SJ, Dodd J (2003) A role for BMP heterodimers in roof plate-mediated repulsion of commissural axons. Neuron 38: 389–401.
9. Snow DM, Steindler DA, Silver J (1990) Molecular and cellular characterization of the glial roof plate of the spinal cord and optic tectum: a possible role for a proteoglycan in the development of an axon barrier. Dev Biol 138: 359–376.
10. Chizhikov VV, Millen KJ (2004) Control of roof plate formation by Lmx1a in the developing spinal cord. Development 131: 2693–2705.
11. García-Lecea M, Kondrychyn I, Fong SH, Ye Z-R, Korzh V (2008) In vivo Analysis of Choroid Plexus Morphogenesis in Zebrafish. PLoS ONE 3: e3090.
12. Papan C, Campos-Ortega JA (1999) Region-specific cell clones in the developing spinal cord of the zebrafish. Dev Genes Evol 209: 135–144.
13. Sevc J, Daxnerová Z, Miklosová M (2009) Role of radial glia in transformation of the primitive lumen to the central canal in the developing rat spinal cord. Cell Mol Neurobiol 29: 927–936.
14. Böhme G (1988) Formation of the central canal and dorsal glial septum in the spinal cord of the domestic cat. J Anat 159: 37–47.

15. Mestres P, Garfia A (1980) Effects of cytochalasin B on the ependyma. Scan Electron Microsc 3: 465–474.
16. Morriss-Kay GM, Tuckett F (1985) The role of microfilaments in cranial neurulation in rat embryos: effects of short-term exposure to cytochalasin D. J Embryol Exp Morph 88: 333–348.
17. Sadler TW, Greenberg D, Coughlin P, Lessard JL (1982) Actin distribution patterns in the mouse neural tube during neurulation. Science 215: 172–174.
18. Smedley MJ, Stanisstreet M (1986) Calcium and neurulation in mammalian embryos. II. Effects of cytoskeletal inhibitors and calcium antagonists on the neural folds of rat embryos. J Embryol Exp Morph 93: 167–178.
19. Li YC, Bai WZ, Sakai K, Hashikawa T (2009) Fluorescence and electron microscopic localization of F-actin in the ependymocytes. J Histochem Cytochem 57: 741–751.
20. Hildebrand JD, Soriano P (1999) Shroom, a PDZ domain-containing actin binding protein, is required for neural tube morphogenesis in mice. Cell 99: 485–497.
21. Nagele RG, Hunter E, Bush K, Lee HY (1987) Studies on the mechanisms of neurulation in the chick: morphometric analysis of force distribution within the neuroepithelium during neural tube formation. J Exp Zool 244: 425–436.
22. Sawyer JM, Harrell JR, Shemer G, Sullivan-Brown J, Roh-Johnson M, et al. (2010) Apical constriction: a cell shape change that can drive morphogenesis. Dev Biol 341: 5–19.
23. Brouns MR, Matheson SF, Hu K-Q, Delalle I, Caviness VS, et al. (2000) The adhesion signaling molecule p190 RhoGAP is required for morphogenetic processes in neural development. Development 127: 4891–4903.
24. Gurniak CB, Perlas E, Witke W (2005) The actin depolymerizing factor cofilin is essential for neural tube morphogenesis and neural crest cell migration. Dev Biol 278: 231–241.
25. Stumpo DJ, Bock CB, Tuttle JS, Blackshear PJ (1995) MARCKS deficiency in mice leads to abnormal brain development and perinatal death. Proc Natl Acad Sci USA 92: 944–948.
26. Wu M, Chen DF, Sasaoka T, Tonegawa S (1996) Neural tube defects and abnormal brain development in F52-deficient mice. Proc Natl Acad Sci USA 93: 21102115.
27. Harris MJ (2001) Why are the genes that cause risk of human neural tube defects so hard to find? Teratology 63: 165–166.
28. Harris MJ, Juriloff DM (2007) Mouse mutants with neural tube closure defects and their role in understanding human neural tube defects. Birth Defects Res A Clin Mol Teratol 79: 187–210.
29. Copp AJ (2005) Neurulation in the cranial region–normal and abnormal. J Anat 207: 623–635.
30. Aruga J (2004) The role of Zic genes in neural development. Mol Cell Neurosci 26: 205–221.
31. Grinberg I, Millen KJ (2005) The ZIC gene family in development and disease. Clin Genet 67: 290–296.
32. Merzdorf CS (2007) Emerging roles for zic genes in early development. Dev Dyn 236: 922–940.
33. Parisi MA, Dobyns WB (2003) Human malformations of the midbrain and hindbrain: review and proposed classification scheme. Mol Genet Metab 80: 36–53.
34. Grinberg I, Northrup H, Ardinger H, Prasad C, Dobyns WB, et al. (2004) Heterozygous deletion of the linked genes ZIC1 and ZIC4 is involved in Dandy-Walker malformation. Nat Genet 36: 1053–1055.
35. Blank MC, Grinberg I, Aryee E, Laliberte C, Chizhikov VV, et al. (2011) Multiple developmental programs are altered by loss of Zic1 and Zic4 to cause Dandy-Walker malformation cerebellar pathogenesis. Development 138: 1207–1216.
36. Elsen GE, Choi LY, Millen KJ, Grinblat Y, Prince VE (2008) Zic1 and Zic4 regulate zebrafish roof plate specification and hindbrain ventricle morphogenesis. Dev Biol 314: 376–392.
37. Nyholm MK, Abdelilah-Seyfried S, Grinblat Y (2009) A novel genetic mechanism regulates dorsolateral hinge-point formation during zebrafish cranial neurulation. J Cell Sci 122: 2137–2148.
38. Parinov S, Kondrichin I, Korzh V, Emelyanov A (2004) Tol2 transposon-mediated enhancer trap to identify developmentally regulated zebrafish genes in vivo. Dev Dyn 231: 449–459.
39. Keller MJ, Chitnis AB (2007) Insights into the evolutionary history of the vertebrate zic3 locus from a teleost-specific zic6 gene in the zebrafish, Danio rerio. Dev Genes Evol 217: 541–547.
40. Kondrychyn I, Garcia-Lecea M, Emelyanov A, Parinov S, Korzh V (2009) Genome-wide analysis of Tol2 transposon reintegration in zebrafish. BMC Genomics 10: 418.
41. Appel B, Givan LA, Eisen JS (2001) Delta-Notch signaling and lateral inhibition in zebrafish spinal cord development. BMC Dev Biol 1: 13.
42. Lyons DA, Guy AT, Clarke JD (2003) Monitoring neural progenitor fate through multiple rounds of division in an intact vertebrate brain. Development 130: 3427–3436.
43. Sturrock RR (1981) An electron microscopic study of the development of the ependyma of the central canal of the mouse spinal cord. J Anat 132: 119–136.
44. Altman J, Bayer SA (1984) The development of the rat spinal cord. Adv Anat Embryol Cell Biol 85: 1–164.
45. Geldmacher-Voss B, Reugels AM, Pauls S, Campos-Ortega JA (2003) A 90degree rotation of the mitotic spindle changes the orientation of mitoses of zebrafish neuroepithelial cells. Development 130: 3767–3780.
46. Brand M, Heisenberg CP, Warga RM, Pelegri F, Karlstrom RO, et al. (1996) Mutations affecting development of the midline and general body shape during zebrafish embryogenesis. Development 123: 129–142.
47. Nakano Y, Kim HR, Kawakami A, Roy S, Schier AF, et al. (2004) Inactivation of dispatched 1 by the chameleon mutation disrupts Hedgehog signalling in the zebrafish embryo. Dev Biol 269: 381–392.
48. Pogoda HM, Solnica-Krezel L, Driever W, Meyer D (2000) The zebrafish forkhead transcription factor FoxH1/Fast1 is a modulator of nodal signaling required for organizer formation. Curr Biol 10: 1041–1049.
49. Wolff C, Roy S, Lewis KE, Schauerte H, Joerg-Rauch G, et al. (2004) iguana encodes a novel zinc-finger protein with coiled-coil domains essential for Hedgehog signal transduction in the zebrafish embryo. Genes Dev 18: 1565–1576.
50. Cui WW, Low SE, Hirata H, Saint-Amant L, Geisler R, et al. (2005) The zebrafish shocked gene encodes a glycine transporter and is essential for the function of early neural circuits in the CNS. J Neurosci 25: 6610–6620.
51. Hansen DV, Lui JH, Parker PR, Kriegstein AR (2010) Neurogenic radial glia in the outer subventricular zone of human neocortex. Nature 464: 554–561.
52. März M, Chapouton P, Diotel N, Vaillant C, Hesl B, et al. (2010) Heterogeneity in progenitor cell subtypes in the ventricular zone of the zebrafish adult telencephalon. Glia 58: 870–888.
53. Jain M, Nilsson R, Sharma S, Madhusudhan N, Kitami T, et al. (2012) Metabolite profiling identifies a key role for glycine in rapid cancer cell proliferation. Science 336: 1040–1044.
54. Locasale JW, Grassian AR, Melman T, Lyssiotis CA, Mattaini KR, et al. (2011) Phosphoglycerate dehydrogenase diverts glycolytic flux and contributes to oncogenesis. Nat Genet 43: 869–874.
55. Zhang WC, Shyh-Chang N, Yang H, Rai A, Umashankar S, et al. (2012) Glycine decarboxylase activity drives non-small cell lung cancer tumor-initiating cells and tumorigenesis. Cell 148: 259–272.
56. Munson C, Huisken J, Bit-Avragim N, Kuo T, Dong PD, et al. (2008) Regulation of neurocoel morphogenesis by Pard6 gamma b. Dev Biol 324: 41–54.
57. Teh C, Chudakov D, Poon KL, Mamedov IZ, Sek JY, et al. (2010) Optogenetic in vivo cell manipulation using KillerRed expressing zebrafish transgenics. BMC Dev Biol 10: 110.
58. Lowery LA, Sive H (2005) Initial formation of zebrafish brain ventricles occurs independently of circulation and requires the nagie oko and snakehead/atp1a1a1 gene products. Development 132: 2057–2067.
59. Ishizaki T, Uehata M, Tamechika I, Keel J, Nonomura K, et al. (2000) Pharmacological properties of Y-27632, a specific inhibitor of rho-associated kinases. Mol Pharmacol 57: 976–983.
60. Kinoshita N, Sasai N, Misaki K, Yonemura S (2008) Apical accumulation of Rho in the neural plate is important for neural plate cell shape change and neural tube formation. Mol Biol Cell 19: 2289–2299.
61. Zhao ZS, Manser E (2005) PAK and other Rho-associated kinases - effectors with surprisingly diverse mechanisms of regulation. Biochem J 386: 201–214.
62. Kimmel CB, Ballard WW, Kimmel SR, Ullmann B, Schilling TF (1995) Stages of embryonic development of the zebrafish. Dev Dyn 203: 253–310.
63. Elmonem ME, Mohamed SA, Aly KH (2007) Early embryonic development of the camel lumbar spinal cord segment. Anat Histol Embryol 36: 43–46.
64. McMahon AR, Merzdorf CS (2010) Expression of the zic1, zic2, zic3, and zic4 genes in early chick embryos. BMC Res Notes 16: 167.
65. Westerfield M (2000) The zebrafish book: A guide for the laboratory use of zebrafish (*Danio rerio*). Eugene: University of Oregon Press. 300 p.
66. Jiang YJ, Brand M, Heisenberg CP, Beuchle D, Furutani-Seiki M, et al. (1996) Mutations affecting neurogenesis and brain morphology in the zebrafish, Danio rerio. Development 123: 205–216.
67. Zhang J, Talbot WS, Schier AF (1998) Positional cloning identifies zebrafish one-eyed pinhead as a permissive EGF-related ligand required during gastrulation. Cell 92: 241–251.
68. Varga ZM, Amores A, Lewis KE, Yan YL, Postlethwait JH, et al. (2001) Zebrafish smoothened functions in ventral neural tube specification and axon tract formation. Development 128: 3497–3509.
69. Schauerte HE, van Eeden FJ, Fricke C, Odenthal J, Strähle U, et al. (1998) Sonic hedgehog is not required for the induction of medial floor plate cells in the zebrafish. Development 125: 2983–2993.
70. Korzh V, Edlund T, Thor S (1993) Zebrafish primary neurons initiate expression of the LIM homeodomain protein Isl-1 at the end of gastrulation. Development 118: 417–425.